Electron-impact ionization of the inner subshells of uranium

M. S. Pindzola
Department of Physics, Auburn University, Auburn, Alabama 36849, USA
(Received 7 July 2014; published 13 August 2014)

Fully relativistic first-order perturbation theory calculations are made for the electron-impact ionization of the inner K, L, and M subshells of uranium. One set of calculations only includes the two-body electrostatic interaction, while the other set includes the full two-body retarded electromagnetic interaction. The K subshell calculations show large differences between the two sets of calculations, the L subshell calculations show moderate differences, and the M subshell calculations show small differences. The M subshell calculations fall within the error bars of recent measurements [A. Moy *et al.*, J. Phys. B **47**, 055202 (2014)].

DOI: 10.1103/PhysRevA.90.022708 PACS number(s): 34.80.Dp

I. INTRODUCTION

Electron-impact ionization of the inner subshells of atoms is a prime mechanism for the production of x rays for many astrophysical objects and laboratory settings. For example, x rays are emitted in heavy metals from neutron star mergers [1]. For the electron-impact excitation and ionization of highly charged atomic ions, perturbative fully relativistic methods [2–5] were developed that included the full two-body retarded electromagnetic interaction. In recent years nonperturbative fully relativistic methods [6–9] have been developed to study the electron-impact excitation and ionization of all atoms and their ions, including the full two-body retarded electromagnetic interaction for the highly charged atomic ions [10].

Motivated by recent measurements [11] for the electron-impact ionization of the M subshells of the U atom, we make perturbative fully relativistic calculations for the K, L, and M subshells. For each subshell, cross sections are calculated when only the two-body electrostatic interaction is included and when the full two-body retarded electromagnetic interaction is included. We also check our K-shell results for the U atom by making calculations for U^{90+} and comparing to an Electron Beam Ion Trap (EBIT) measurement [12] made 20 years ago. We hope that our calculations inspire further deep inner-shell measurements for U and other heavy atoms.

The rest of this paper is organized as follows. In Sec. II we review the theoretical method. The subconfiguration-average ionization cross section is introduced first, and then detailed expressions are given in Sec. II A for the scattering probabilities when only the two-body electrostatic interaction is included and in Sec. II B for the scattering probabilities when the full two-body retarded electromagnetic interaction is included. In Sec. III cross-section results for the ionization of U^{90+} and the K, L, and M subshells of the U atom are presented and compared with experiment where available. We conclude with a brief summary and future plans in Sec. IV. Unless otherwise stated, we will use atomic units.

II. THEORY

For direct ionization a general transition between relativistic subconfigurations has the form

$$(n_0 l_0 j_0)^{w_0} p_i l_i j_i \rightarrow (n_0 l_0 j_0)^{w_0-1} p_e l_e j_e p_f l_f j_f, \tag{1}$$

where w_0 is a subshell occupation number, $n_0 l_0 j_0$ are quantum numbers of the bound electron, and $p_i l_i j_i$, $p_e l_e j_e$, and $p_f l_f j_f$ are quantum numbers of the initial, ejected, and final continuum electrons. The subconfiguration-average ionization cross section is given by [13]

$$\sigma_{\rm dir} = \frac{16 w_0}{p_i^3} \int_0^{E/2} \frac{d(\epsilon_e)}{p_e p_f} \sum_{l_i,l_e,l_f} \sum_{j_i,j_e,j_f} (2j_i+1)(2j_e+1) \times (2j_f+1) \mathcal{S}(n_0 l_0 j_0 p_i l_i j_i \rightarrow p_e l_e j_e p_f l_f j_f), \tag{2}$$

where $p = \sqrt{2\epsilon + \epsilon^2/c^2}$ and the continuum normalization is $\sqrt{1+\epsilon/2c^2}$ times a sine function.

A. Electrostatic interaction

Using first-order perturbation theory with only the two-body electrostatic interaction, the scattering probabilities are given by [3]

$$\begin{aligned}\mathcal{S}(0i \rightarrow ef) &= \sum_{\lambda} \frac{F(\lambda)F(\lambda)}{(2j_i+1)(2j_f+1)(2j_e+1)(2j_0+1)(2\lambda+1)} \\ &+ \sum_{\lambda'} \frac{G(\lambda')G(\lambda')}{(2j_i+1)(2j_f+1)(2j_e+1)(2j_0+1)(2\lambda'+1)} \\ &+ 2\sum_{\lambda,\lambda'} (-1)^{\lambda+\lambda'} \begin{pmatrix} j_f & j_i & \lambda \\ j_e & j_0 & \lambda' \end{pmatrix} \\ &\times \frac{F(\lambda)G(\lambda')}{(2j_i+1)(2j_f+1)(2j_e+1)(2j_0+1)},\end{aligned} \tag{3}$$

where the direct multipole function

$$F(\lambda) = \bar{R}_\lambda(0i \rightarrow ef) \langle \kappa_f || C^\lambda || \kappa_i \rangle \langle \kappa_e || C^\lambda || \kappa_0 \rangle, \tag{4}$$

the exchange multipole function

$$G(\lambda) = \bar{R}_\lambda(0i \rightarrow fe) \langle \kappa_e || C^\lambda || \kappa_i \rangle \langle \kappa_f || C^\lambda || \kappa_0 \rangle, \tag{5}$$

and $\kappa = -2(j-l)(j+\frac{1}{2})$. The C tensor reduced matrix elements are given by

$$\langle \kappa || C^\lambda || \kappa' \rangle = (-1)^{j-\frac{1}{2}} \sqrt{(2j+1)(2j'+1)} \begin{pmatrix} j & \lambda & j' \\ \frac{1}{2} & 0 & -\frac{1}{2} \end{pmatrix}, \tag{6}$$

provided $l + l' + \lambda$ is even, and are otherwise zero. The radial two-body electrostatic integrals are given by

$$\bar{R}_\lambda(0i \to ef) = \int_0^\infty dr \int_0^\infty dr' \frac{r_<^\lambda}{r_>^{\lambda+1}} \times [P_0(r)P_e(r) + Q_0(r)Q_e(r)] \times [P_i(r')P_f(r') + Q_i(r')Q_f(r')], \quad (7)$$

where $P(r)$ and $Q(r)$ are the large and small components of the Dirac spinor for the radial bound and continuum solutions. The energies and bound radial orbitals are calculated using Grant's atomic structure package [14,15], while the continuum radial orbitals are obtained by solving the single-channel Dirac equation given by

$$\left(\frac{d}{dr} + \frac{\kappa}{r}\right) P(r) + \frac{1}{c}[V_n(r) - \epsilon - 2c^2 + V_{DF}]Q(r) = 0, \quad (8)$$

$$\left(\frac{d}{dr} - \frac{\kappa}{r}\right) Q(r) - \frac{1}{c}[V_n(r) - \epsilon + V_{DF}]P(r) = 0, \quad (9)$$

where $V_n(r)$ is the nuclear potential and the distorting potential operator V_{DF} is constructed from the atomic structure bound radial orbitals.

B. Retarded electromagnetic interaction

Using first-order perturbation theory with the full two-body retarded electromagnetic interaction, the scattering probabilities are given by [3]

$$\begin{aligned}\mathcal{S}(0i \to ef) &= \sum_{\lambda,\lambda'}\sum_{\Lambda} \frac{(-1)^{\lambda+\lambda'} F(\lambda,\Lambda)F^*(\lambda',\Lambda)}{(2j_i+1)(2j_f+1)(2j_e+1)(2j_0+1)(2\Lambda+1)} \\ &+ \sum_{\lambda,\lambda'}\sum_{\Lambda} \frac{(-1)^{\lambda+\lambda'} G(\lambda,\Lambda)G^*(\lambda',\Lambda)}{(2j_i+1)(2j_f+1)(2j_e+1)(2j_0+1)(2\Lambda+1)} \\ &+ 2\sum_{\lambda,\lambda'}\sum_{\Lambda,\Lambda'} (-1)^{\lambda+\lambda'} \begin{pmatrix} j_f & j_i & \Lambda \\ j_e & j_0 & \Lambda' \end{pmatrix} \\ &\times \frac{\mathrm{Re}[F(\lambda,\Lambda)G^*(\lambda',\Lambda')]}{(2j_i+1)(2j_f+1)(2j_e+1)(2j_0+1)}, \end{aligned} \quad (10)$$

where the direct multipole function

$$\begin{aligned} F(\lambda,\Lambda) &= R_\lambda(0i \to ef)\delta_{\lambda,\Lambda}\langle\kappa_f||C^\lambda||\kappa_i\rangle\langle\kappa_e||C^\lambda||\kappa_0\rangle \\ &- S_\lambda^1(0i \to ef)\delta(1\lambda\Lambda)\langle\kappa_f||V^\Lambda||-\kappa_i\rangle\langle\kappa_e||V^\Lambda||-\kappa_0\rangle \\ &+ S_\lambda^2(0i \to ef)\delta(1\lambda\Lambda)\langle\kappa_f||V^\Lambda||-\kappa_i\rangle\langle-\kappa_e||V^\Lambda||\kappa_0\rangle \\ &+ S_\lambda^3(0i \to ef)\delta(1\lambda\Lambda)\langle-\kappa_f||V^\Lambda||\kappa_i\rangle\langle\kappa_e||V^\Lambda||-\kappa_0\rangle \\ &- S_\lambda^4(0i \to ef)\delta(1\lambda\Lambda)\langle-\kappa_f||V^\Lambda||\kappa_i\rangle\langle-\kappa_e||V^\Lambda||\kappa_0\rangle \end{aligned} \quad (11)$$

and the exchange multipole function

$$\begin{aligned} G(\lambda,\Lambda) &= R_\lambda(0i \to fe)\delta_{\lambda,\Lambda}\langle\kappa_e||C^\lambda||\kappa_i\rangle\langle\kappa_f||C^\lambda||\kappa_0\rangle \\ &- S_\lambda^1(0i \to fe)\delta(1\lambda\Lambda)\langle\kappa_e||V^\Lambda||-\kappa_i\rangle\langle\kappa_f||V^\Lambda||-\kappa_0\rangle \\ &+ S_\lambda^2(0i \to fe)\delta(1\lambda\Lambda)\langle\kappa_e||V^\Lambda||-\kappa_i\rangle\langle-\kappa_f||V^\Lambda||\kappa_0\rangle \\ &+ S_\lambda^3(0i \to fe)\delta(1\lambda\Lambda)\langle-\kappa_e||V^\Lambda||\kappa_i\rangle\langle\kappa_f||V^\Lambda||-\kappa_0\rangle \\ &- S_\lambda^4(0i \to fe)\delta(1\lambda\Lambda)\langle-\kappa_e||V^\Lambda||\kappa_i\rangle\langle-\kappa_f||V^\Lambda||\kappa_0\rangle. \end{aligned} \quad (12)$$

The V tensor reduced matrix elements are given by

$$\begin{aligned}&\langle\kappa||V^\Lambda||\kappa'\rangle \\ &= (-1)^l\sqrt{6(2l+1)(2l'+1)(2j+1)(2j'+1)(2\Lambda+1)} \\ &\times \begin{pmatrix} l & \lambda & l' \\ 0 & 0 & 0 \end{pmatrix} \begin{Bmatrix} l & \frac{1}{2} & j \\ l' & \frac{1}{2} & j' \\ \lambda & 1 & \Lambda \end{Bmatrix}, \end{aligned} \quad (13)$$

which may be reduced to a single $3j$ symbol [16]. The radial two-body retarded electromagnetic integrals are given by

$$R_\lambda(0i \to ef) = \int_0^\infty dr \int_0^\infty dr'(2\lambda+1)\xi j_\lambda(\xi r_>)h_\lambda^+(\xi r_>) \times [P_0(r)P_e(r) + Q_0(r)Q_e(r)] \times [P_i(r')P_f(r') + Q_i(r')Q_f(r')], \quad (14)$$

$$S_\lambda^1(0i \to ef) = \int_0^\infty dr \int_0^\infty dr'(2\lambda+1)\xi j_\lambda(\xi r_>)h_\lambda^+(\xi r_>) \times [P_0(r)Q_e(r)P_i(r')Q_f(r')], \quad (15)$$

$$S_\lambda^2(0i \to ef) = \int_0^\infty dr \int_0^\infty dr'(2\lambda+1)\xi j_\lambda(\xi r_>)h_\lambda^+(\xi r_>) \times [P_0(r)Q_e(r)Q_i(r')P_f(r')], \quad (16)$$

$$S_\lambda^3(0i \to ef) = \int_0^\infty dr \int_0^\infty dr'(2\lambda+1)\xi j_\lambda(\xi r_>)h_\lambda^+(\xi r_>) \times [Q_0(r)P_e(r)P_i(r')Q_f(r')], \quad (17)$$

$$S_\lambda^4(0i \to ef) = \int_0^\infty dr \int_0^\infty dr'(2\lambda+1)\xi j_\lambda(\xi r_>)h_\lambda^+(\xi r_>) \times [Q_0(r)P_e(r)Q_i(r')P(r')], \quad (18)$$

where $j_\lambda(x)$ and $h_\lambda^+(x)$ are spherical Bessel functions and $\xi = (\epsilon_f - \epsilon_i)/c$.

TABLE I. Uranium ground configuration ionization potentials.

Subshell	Orbital	Ionization potential (keV)
$K1$	$1s^2$	116.4
$L1$	$2s^2$	21.9
$L2$	$2\bar{p}^2$	21.1
$L3$	$2p^4$	17.3
$M1$	$3s^2$	5.62
$M2$	$3\bar{p}^2$	5.25
$M3$	$3p^4$	4.36
$M4$	$3\bar{d}^4$	3.78
$M5$	$3d^6$	3.60

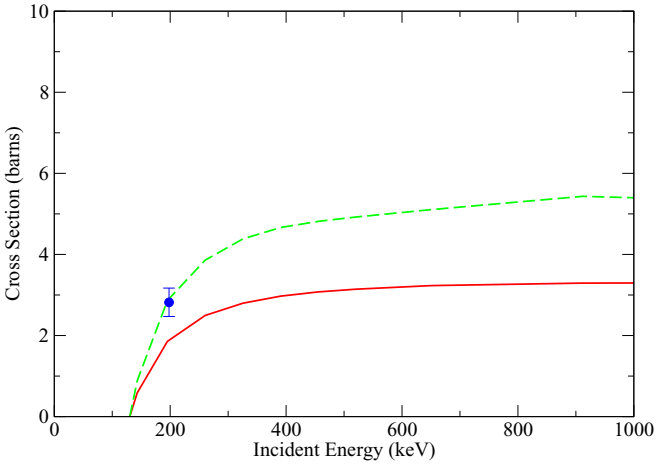

FIG. 1. (Color online) Electron-impact ionization of U^{90+}. Solid red line, SCADW electrostatic; dashed green line, SCADW retarded electromagnetic; blue circle with error bar, experiment [12] ($1.0\ \text{b} = 1.0\times10^{-24}\ \text{cm}^2$).

III. RESULTS

Subconfiguration-average distorted-wave (SCADW) calculations based on Eq. (2) are first made for the electron-impact ionization of U^{90+}. The $1s^2$ ground subconfiguration of U^{90+} is calculated using Grant's atomic structure package [14,15] and is found to have an ionization potential of 130.2 keV. The SCADW results for U^{90+} are presented in Fig. 1. The SCADW results including the full two-body retarded electromagnetic interaction are in good agreement with an EBIT measurement [12] at 198.0 keV. We note that relativistic distorted-wave calculations including the Breit interaction by Fontes *et al.* [5] are also in good agreement with experiment [12] at 198.0 keV.

SCADW calculations based on Eq. (2) are then made for the electron-impact ionization of the U atom. The

$$1s^2 2s^2 2\bar{p}^2 2p^4 3s^2 3\bar{p}^2 3p^4 3\bar{d}^4 3d^6 4s^2 4\bar{p}^2 4p^4 4\bar{d}^4 4d^6$$
$$4\bar{f}^6 4f^8 5s^2 5\bar{p}^2 5p^4 5\bar{d}^4 5d^6 5\bar{f}^3 6s^2 6\bar{p}^2 6p^4 6\bar{d} 7s^2$$

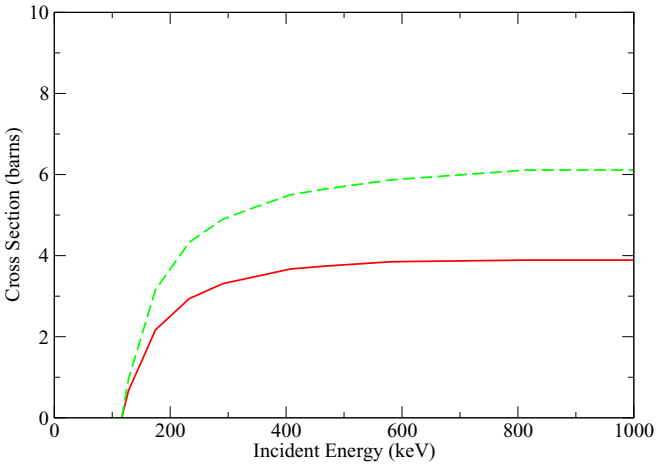

FIG. 2. (Color online) Electron-impact ionization of the $K1$ subshell of uranium. Solid red line, SCADW electrostatic;dashed green line, SCADW retarded electromagnetic ($1.0\ \text{b} = 1.0\times10^{-24}\ \text{cm}^2$).

ground subconfiguration of U is calculated using Grant's atomic structure package [14,15] and is found to have the ionization potentials for the K, L, and M subshells given

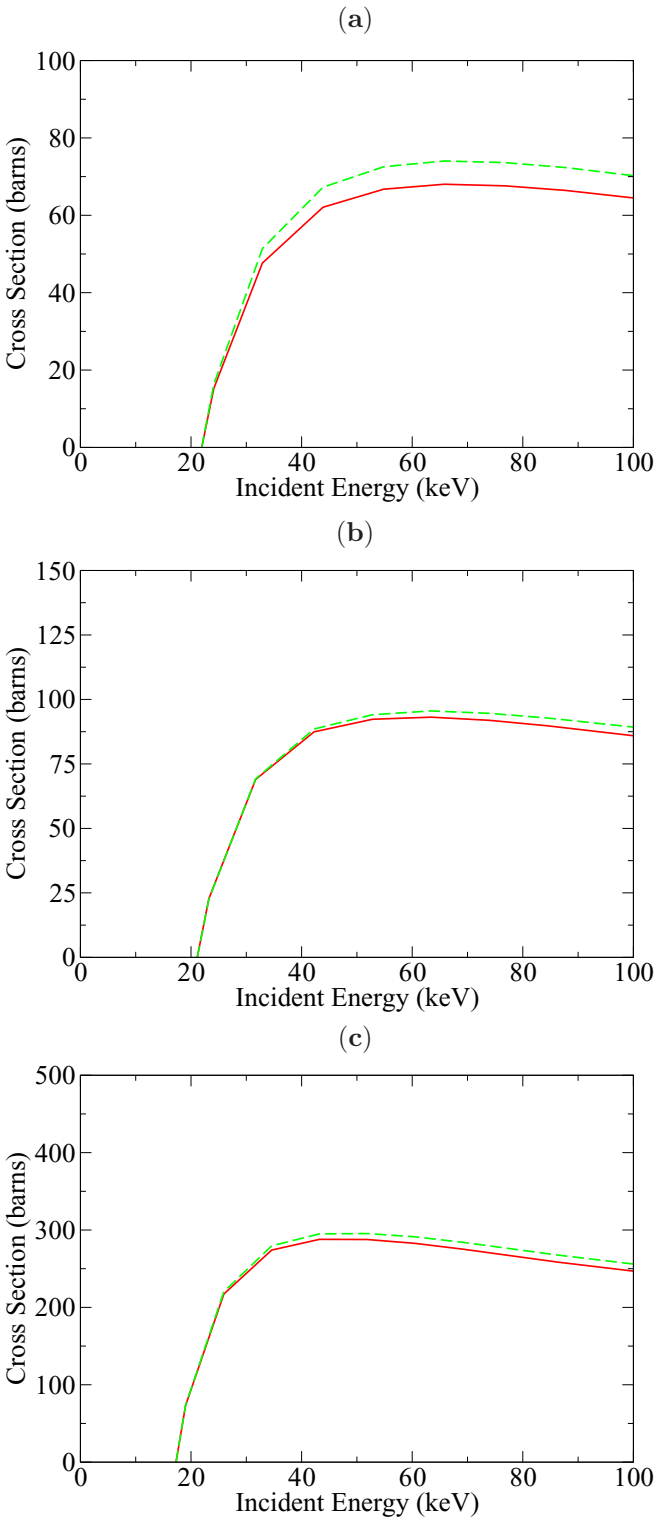

FIG. 3. (Color online) Electron-impact ionization of the L subshells of uranium: (a) $L1$, (b) $L2$, and (c) $L3$. Solid red line, SCADW electrostatic; dashed green line, SCADW retarded electromagnetic ($1.0\ \text{b} = 1.0\times10^{-24}\ \text{cm}^2$).

in Table I. The SCADW results for the K subshell of U are presented in Fig. 2. When compared to the SCADW results for U^{90+}, the K subshell results for U are slightly larger due to the screening effects of the L subshell electrons. In both Figs. 1 and 2 there are large differences between the two-body electrostatic interaction calculations and the full two-body retarded electromagnetic interaction calculations.

SCADW calculations based on Eq. (2) for the L subshells of U are presented in Fig. 3, and those for the M subshells of U are shown in Fig. 4. The differences between the two-body electrostatic interaction and the full two-body retarded electromagnetic interaction calculations are only moderate for the L subshells and small for the M subshells. The SCADW results for the electron-impact ionization of the M subshells of U all fall within the error bars of recent measurements [11]. We note that relativistic distorted-wave calculations by Bote and Salvat [17] are also in good agreement with experiment [11].

IV. SUMMARY

We have carried out fully relativistic first-order perturbation theory calculations for the electron-impact ionization of

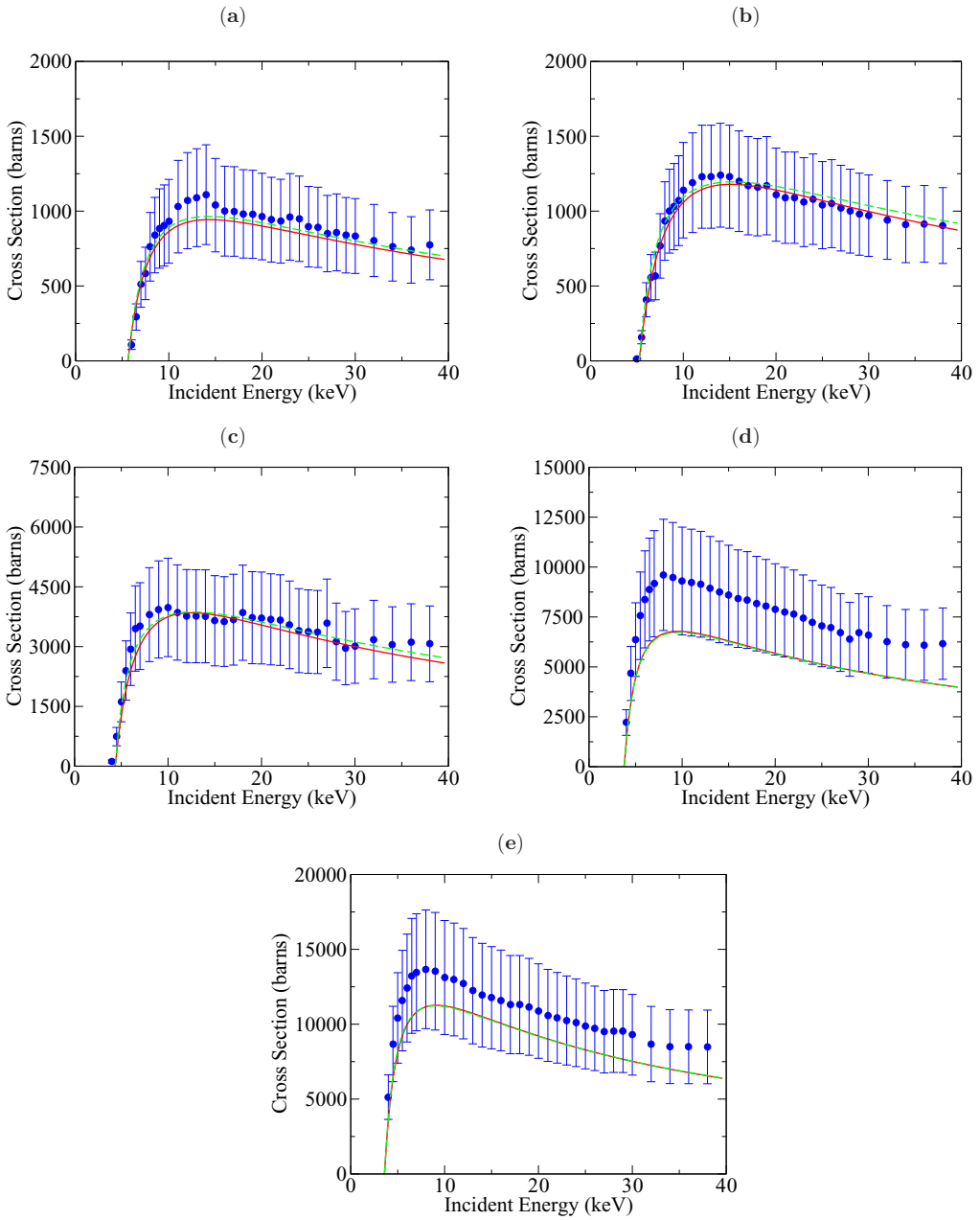

FIG. 4. (Color online) Electron-impact ionization of the M subshells of uranium: (a) $M1$, (b) $M2$, (c) $M3$, (d) $M4$, and (e) $M5$. Solid red line, SCADW electrostatic; dashed green line, SCADW retarded electromagnetic; blue circles with error bars, experiment [11] ($1.0\ \mathrm{b} = 1.0\times10^{-24}\ \mathrm{cm}^2$).

the K, L, and M subshells of the U atom. Differences between calculations that include only two-body electrostatic interactions and those that include the full two-body retarded electromagnetic interactions become smaller as one progresses from the $K1$ subshell to the $M5$ subshell. The M subshell calculations all fall within the error bars of recent measurements. We hope that our calculations for the K and L subshells of U will inspire further electron-impact ionization cross-section measurements for U and other heavy atoms.

ACKNOWLEDGMENTS

We would like to thank C. P. Ballance at Auburn University and C. J. Fontes at Los Alamos National Laboratory for useful discussions. This work was supported in part by grants from the US Department of Energy and the US National Science Foundation. Computational work was carried out at the National Energy Research Scientific Computing Center in Oakland, California, and the National Center for Computational Sciences in Oak Ridge, Tennessee.

[1] D. Kasen, N. R. Badnell, and J. Barnes, Astrophys. J. **774**, 25 (2013).
[2] D. W. Walker, J. Phys. B **8**, 760 (1975).
[3] M. S. Pindzola, D. L. Moores, and D. C. Griffin, Phys. Rev. A **40**, 4941 (1989).
[4] C. J. Fontes, D. H. Sampson, and H. L. Zhang, Phys. Rev. A **47**, 1009 (1993).
[5] C. J. Fontes, D. H. Sampson, and H. L. Zhang, Phys. Rev. A **51**, R12 (1995).
[6] D. V. Fursa and I. Bray, Phys. Rev. Lett. **100**, 113201 (2008).
[7] O. Zatsarinny and K. Bartschat, Phys. Rev. A **77**, 062701 (2008).
[8] N. R. Badnell, J. Phys. B **41**, 175202 (2008).
[9] M. S. Pindzola, J. A. Ludlow, F. Robicheaux, J. Colgan, and C. J. Fontes, Phys. Rev. A **80**, 052706 (2009).
[10] C. J. Bostock, D. V. Fursa, and I. Bray, Phys. Rev. A **86**, 042709 (2012).
[11] A. Moy, C. Merlet, X. Liovet, and O. Dugne, J. Phys. B **47**, 055202 (2014).
[12] R. E. Marrs, S. R. Elliott, and D. A. Knapp, Phys. Rev. Lett. **72**, 4082 (1994).
[13] M. S. Pindzola and M. J. Buie, Phys. Rev. A **37**, 3232 (1988).
[14] I. P. Grant, *Relativistic Quantum Theory of Atoms and Molecules* (Springer, New York, 2007).
[15] K. G. Dyall, I. P. Grant, C. T. Johnson, F. A. Parpia, and E. P. Plummer, Comput. Phys. Commun. **55**, 425 (1989).
[16] D. M. Brink and G. R. Satchler, *Angular Momentum* (Clarendon, Oxford, 1968).
[17] D. Bote and F. Salvat, Phys. Rev. A **77**, 042701 (2008).